

**FABRICATION AND MEASUREMENT OF HIGH T_c
SUPERCONDUCTING MICROBOLOMETERS***

M. Nahum, Qing Hu,^{a)} and P. L. Richards

Department of Physics, University of California at Berkeley,
and Materials and Chemical Sciences Division, Lawrence Berkeley Laboratory,
Berkeley, CA 94720.

and

S. A. Sachtjen, N. Newman, and B. F. Cole

Conductus, Inc., 969 West Maude Ave., Sunnyvale, CA 94086.

^{a)} Present address: Department of Electrical Engineering and Computer Science and Research Laboratory of Electronics, MIT.

* This work was supported by the Director, Office of Energy Research, Office of Basic Energy Sciences, Material Sciences Division, of the U. S. Department of Energy under Contract No. DE-AC03-76SF00098.

MASTER

DISTRIBUTION OF THIS DOCUMENT IS UNLIMITED

FABRICATION AND MEASUREMENT OF
HIGH T_c SUPERCONDUCTING MICROBOLOMETERS*

M. Nahum, Qing Hu†, and P. L. Richards.
Department of Physics, University of California at Berkeley,
and Materials and Chemical Sciences division, Lawrence Berkeley Laboratory,
Berkeley, CA 94720.

and
S. A. Sachtjen, N. Newman and B. F. Cole
Conductus, Inc.,
969 West Maude Ave.
Sunnyvale, CA 94086.

Abstract

We have fabricated and measured the performance of antenna-coupled microbolometers based on the resistive transition of a high T_c superconducting film for use as detectors of far-infrared and millimeter waves. A planar lithographed antenna (log-periodic or log-spiral) is used to couple the radiation to a thin YBCO film with dimensions ($\approx 6 \times 13 \mu\text{m}^2$) which are much smaller than the wavelength to be measured. This film acts both as the resistor to thermalize the RF currents and as a transition edge thermometer to measure the resulting temperature rise. Because of its small size, both the thermal conductance from the film into the bulk of the substrate and the heat capacity of the thermally active region are small. Consequently, the microbolometer has low noise, fast response and a high voltage responsivity. We have measured a phonon limited electrical NEP of $4.5 \times 10^{-12} \text{ WHz}^{-1/2}$ at 10 kHz modulation frequency and a responsivity of 478 V/W at a bias of 550 μA . Measurements of the optical efficiency are in progress and will be discussed.

Introduction

The discovery of high T_c superconductivity offers the possibility of constructing sensitive transition edge bolometers for use as detectors of far infrared and millimeter waves. These detectors are intended to bridge the gap between liquid helium cooled bolometers and room temperature detectors such as the Golay cell, the pyroelectric detector and the bismuth microbolometer. Recent estimates^{1,2} indicate that high T_c bolometric detectors can potentially be two orders of magnitude more sensitive than any competing direct detector at or above liquid-nitrogen temperatures for infrared wavelengths longer than 20 μm . In what follows, we summarize the expected thermal behavior of the high T_c microbolometer, then we discuss the fabrication procedures, the electrical and optical characterization and finally measurements of the efficiency of the quasi-optical coupling scheme.

Operating Principles

Thermal Isolation

Following the analysis of Ref. 2, the thermal conductance G_s from the superconducting film to the bulk of the substrate can be written as

$$G_s(f) = \frac{\kappa_s}{\Delta T} \int_{A_{ca}} \nabla T(r) \cdot ds \quad (1)$$

where κ_s is the thermal conductivity of the substrate, $T(r)$ is the position dependent temperature in the substrate, ΔT is the temperature difference between the film and the substrate far from the film, and the integral is over the contact area between the film and the substrate. If we model the contact as a hemisphere of radius a such that $A=2\pi a^2$ is the area of the film, then the radial diffusion equation gives

$$T = T_0 + \Delta T \frac{a}{r} e^{-(a+r)/L} e^{i(2\pi f t - r/L)} \quad (2)$$

where $L = (\kappa_s/c_s \pi f)^{1/2}$ is the thermal diffusion length, c_s is the substrate heat capacity per unit volume, and f is the modulation frequency. The frequency dependent thermal conductance is then given by

$$G_s(f) = \kappa_s \sqrt{2\pi A} [(1 + \sqrt{rf})^2 + \tau f]^{1/2} \quad (3)$$

where $\tau = c_s A / 2\kappa_s$ is an effective time constant. At low frequencies, $G_s(0)$ is frequency independent while at high frequencies ($f \gg \tau$), $G \propto f^{1/2}$. This increase of G_s degrades the sensitivity of the microbolometer at high modulation frequencies.

The contact area between the superconducting thermometer and the antenna edges provides an alternate path for heat dissipation. This additional contribution to the total thermal conductance is difficult to calculate precisely. However, previous estimates³ and present measurements indicate that this is not the dominant thermal conduction path.

Radiation Coupling

It has long been recognized that millimeter to far infrared radiation can be coupled to very small devices by means of an antenna.⁴ Planar lithographed antennas such as log-periodic⁵ and log-spirals⁶ are very attractive candidates for our applications. These antennas are self complementary in that the shape of the regions covered by metal is the same as the regions of bare dielectric. These self complementary antennas are all very broadband and have a frequency independent real antenna impedance $R = 377[2(1+\epsilon)]^{-1/2} \Omega$ that depends only on the dielectric constant ϵ of the substrate. For the substrate choice discussed below this impedance is $\approx 77 \Omega$. The short wavelength behavior of these devices is not well understood but response has been observed at 119 μm .³ Since planar antennas located on a dielectric surface

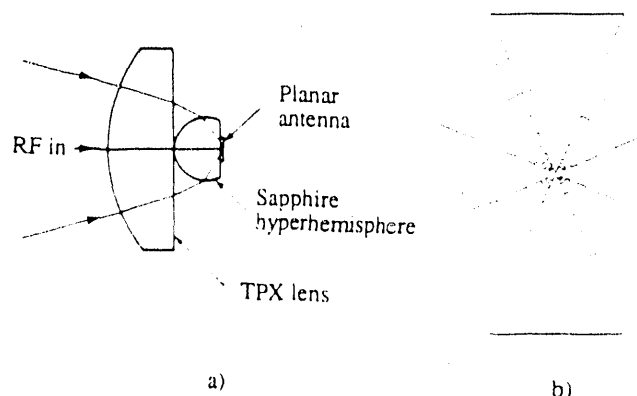


Figure 1. Quasi-optical coupling scheme. a) Cross section. The substrate is mounted on the flat side of a hyperhemispherical sapphire lens ($D=0.5''$). A TPX lens ($f/1.16$) is used to further narrow the beam. b) Planar log-periodic antenna. This self complementary structure gives a frequency independent real antenna impedance and very broadband response. In addition, it has a nearly Gaussian beam pattern.

radiate primarily into the dielectric, the signals are introduced through the back surface of the dielectric which is often placed on the back side of a dielectric lens, as shown in Fig. (1). The efficiency of this quasi-optical coupling scheme has been estimated at 50% and higher.^{5,6}

Detector Performance

If we model the thermal circuit as a heat capacity C coupled to a heat bath through a conductance $G(f)$, then the voltage responsivity is given by

$$S = \frac{I dR/dT}{G(f) + 2\pi f C} \quad (4)$$

where I is the bias current, dR/dT is the temperature coefficient of resistance and f is the modulation frequency. The second term in the denominator can be neglected because of the small thermal mass of the film. To avoid thermal runaway, the current bias must satisfy

$$\alpha \equiv \frac{I^2 dR/dT}{G(f)} < 1 \quad (5)$$

For design purposes we pick a nominal value of $\alpha=0.3$.

The optical NEP of the device is computed by summing the squares of statistically independent contributions

$$NEP = \frac{1}{\eta} \left[4k_B T^2 G(f) + \frac{4k_B T R}{|S|^2} + (NEP)_{1/f}^2 + \frac{4k_B T_n R}{|S|^2} \right]^{1/2} \quad (6)$$

where η is the optical efficiency. The first term is the phonon noise in the device, the second term is the Johnson noise in the resistance R of the film at the midpoint of the transition, the third term is the $1/f$ noise in the film and the last term is the noise from an amplifier with noise temperature T_n . The last two terms can be neglected if we operate at high enough frequencies to avoid the $1/f$ noise in the film and if we use a low noise amplifier (commercially available low noise amplifiers with a typical noise voltage of $1.2 \text{ nVHz}^{-1/2}$ are adequate).

Fabrication

In order to maximize the sensitivity of the microbolometer several conditions must be met. First, the resistance of the superconducting thermometer (when maintained at the center of the resistive transition) must match the antenna impedance of $\approx 77 \Omega$. Since high quality films of YBCO have typical resistivities of $\approx 100 \mu\Omega \text{ cm}$ just above the transition, moderate film thicknesses ($\approx 1000 \text{ \AA}$) are required. The second requirement is that of a low thermal conductivity substrate which is simultaneously compatible with YBCO and is not lossy at infrared frequencies. ZrO_2 stabilized with Y_2O_3 (YSZ) has favorable thermal and film growth properties. It has a thermal conductivity $\kappa_s = 0.015 \text{ Wcm}^{-1}\text{K}^{-1}$,⁷ a specific heat $c_s = 0.7 \text{ Jcm}^{-3}\text{K}^{-1}$,⁸ and a dielectric constant $\epsilon = 12.5$.⁹

In situ, off axis sputtered YBCO films ($\approx 1000 \text{ \AA}$ thick) were deposited on YSZ (the deposition parameters have been discussed elsewhere).¹⁰ Subsequently, $\approx 2500 \text{ \AA}$ of silver were deposited without breaking vacuum. The antenna pattern was defined using standard photolithographic techniques and the silver was etched in a $1\text{H}_2\text{O}_2:1\text{NH}_4\text{O}_3:2\text{CH}_3\text{O}_4$ solution. The YBCO microbridge was then defined and etched in a $\approx 0.5\%$ phosphoric acid etch. The resulting structure has an active area of $\approx 6 \times 13 \mu\text{m}^2$ with a transition width of $\approx 2 \text{ K}$ and $\approx 40 \Omega$ resistance at the center of the transition (Fig.2). The substrate is mounted onto the back side of the hyperhemispherical sapphire lens with Apiezon N-grease and electrical contacts are made at the antenna terminals with silver paint. The substrate-lens combination is temperature regulated at the center of the resistive transition using a commercial diode thermometer and controller.

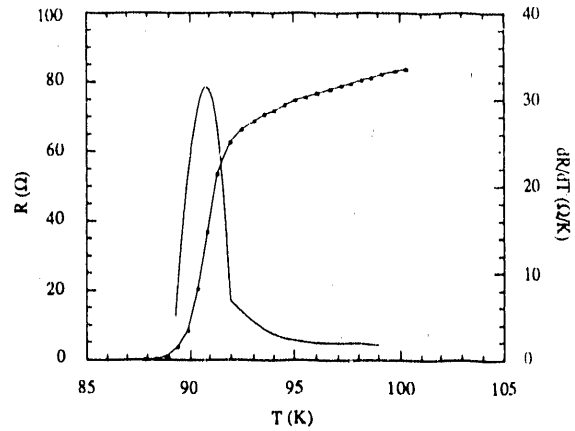


Figure 2. Temperature dependence of the resistance of a typical microbolometer (measured at a bias of $100 \mu\text{A}$), also plotted is the temperature coefficient of resistance whose maximum gives the optimum operating temperature.

Electrical and Optical Characterization

In order to accurately calibrate the responsivity of the microbolometer it is necessary to measure the total thermal conductance out of the thermally active region. This information is contained in the dc I-V curve: The electrical power dissipated in the thermometer raises its temperature which results in a higher resistance. A simple analysis shows that

$$R = R_0 + \frac{dR/dT}{G(0)} I^2 R \quad (7)$$

where R_0 is the resistance at low bias current.

When the temperature was regulated at the center of the transition, a strong linear dependence of the resistance on the bias current was observed. This non thermal behavior dominates the thermal effects. Thus, I-V curves were measured just above the resistive transition.¹¹ Fig. 3 shows a typical resistance versus power load curve. The slight curvature is due to the change in dR/dT as the thermometer changes temperature. From the slope we obtain $G(0) = 3.6 \times 10^{-5} \text{ W/K}$, while the simple thermal model gives a value of $3.3 \times 10^{-5} \text{ W/K}$. The difference may be due to conduction through the antenna.

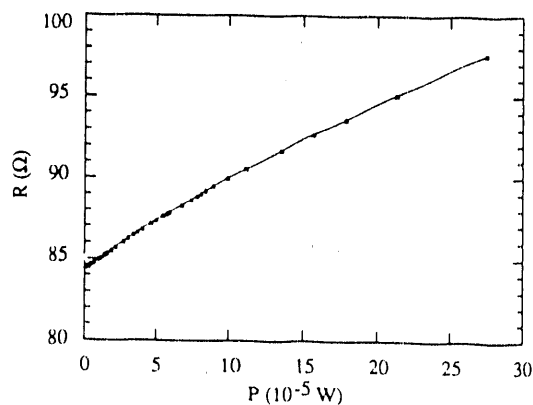


Figure 3. Resistance versus power load curve measured just above the resistive transition. It provides an accurate calibration of the responsivity of the microbolometer.

The electrical NEP (output noise voltage divided by the responsivity) was measured as a function of bias current and frequency. Fig. 4 is a plot of the electrical NEP as a function of bias current at a 10 kHz modulation frequency. Superposed is the expected NEP (assuming unity optical efficiency and zero $1/f$ and

amplifier noise). The solid line is the theoretical phonon noise limit. Since the sensitivity of these microbolometers is limited by phonon noise, their performance may be improved by reducing the dimensions of the active region and, if possible, by creating a thermal boundary resistance layer between the film and the substrate.

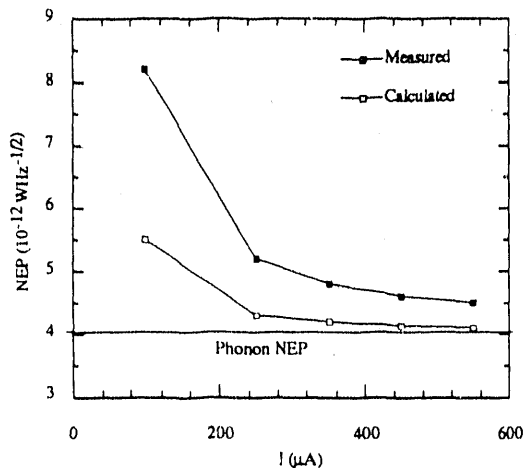


Figure 4. The measured and calculated electrical NEP at a 10 kHz modulation frequency. The sensitivity is limited by thermal fluctuations in the superconducting thermometer.

In Fig. 5 we plot the electrical NEP as a function of modulation frequency for a bias current of 500 μA . The solid line is the expected NEP in the absence of $1/f$ and amplifier noise. Because the $1/f$ noise characteristics at low frequencies are influenced by the deposition and fabrication techniques, improved techniques (such as a dry etch technique and a post fabrication, O_2 anneal) may improve the low frequency noise characteristics and also sharpen the resistive transition.

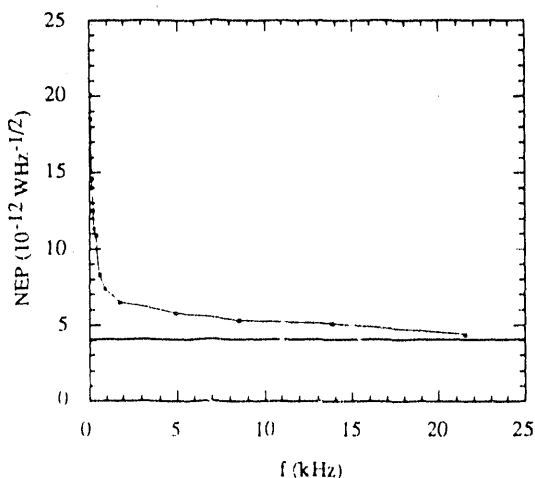


Figure 5. Frequency dependence of the electrical NEP measured at a bias of 100 μA and at the optimum operating temperature. The solid line is the calculated NEP in the absence of $1/f$ noise.

Optical measurements were made with a 90 GHz Gunn oscillator, the frequency modulation was obtained by electrical switching of the oscillator bias. In Fig. 6 we plot the optical response as a function of modulation frequency as well as the response calculated from the simplified thermal model. The discrepancy might be due to thermal conduction through the antenna.

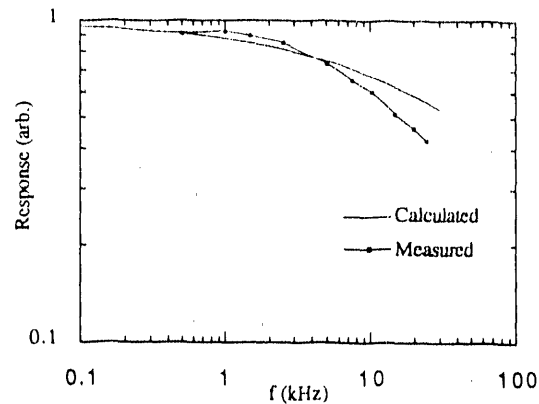


Figure 6. Frequency response of a typical microbolometer at 90 GHz.

Optical Efficiency Measurements

In order to accurately measure the optical efficiency, it is necessary to have a well calibrated source. In addition, the beam patterns of both the source and the detector must be known so that no losses occur in coupling them. A black-body source appears to be a convenient choice. The power output (in the Rayleigh-Jeans limit) is given by $P = k_B T B$ where B is the optical bandwidth. In addition, it is only necessary for the radiation to fill the beam in order to avoid coupling losses. In our configuration, a sheet of Ecosorb AN72, immersed in liquid nitrogen, serves as a 77 K blackbody source. The optical bandwidth B is determined by cooled fused quartz and black polyethylene filters, at the cryostat entrance, which had a measured effective bandwidth of 1.5 THz (50 cm^{-1}). Thus, when chopped between 77 K and room temperature, the incident power is $P = 4.5 \times 10^{-9} \text{ W}$. The integrated optical efficiency, defined as the ratio of the detected power to the incident power (at the TPX lens) was measured to be 5%. This indicates that the losses in the lens and antenna system were 13 dB over the frequency range ($0-50 \text{ cm}^{-1}$) of the observation, compared with the theoretical losses of $\approx 3 \text{ dB}$. The observed losses can be accounted for as follows. The TPX lens had a measured frequency independent loss of 1 dB. The losses of the YSZ/Apiezon N-grease/Sapphire lens combination were measured to be 9 dB when normalized to the optical bandwidth. The main source of loss is in the YSZ substrate (0.5 mm thick) whose transmission becomes negligible at $\approx 30 \text{ cm}^{-1}$. Significant improvements in the optical efficiency appear possible. Since the majority of the losses are due to absorption in the substrate, the use of a thinned YSZ substrate should reduce these losses. In addition, the use of reflecting optics, and perhaps a quartz lens should reduce the losses in the TPX lens and broaden the optical bandwidth (quartz is less lossy than sapphire at $\approx 100 \text{ cm}^{-1}$). A better overall approach would be to deposit the antenna and the sensing element on a thin membrane. Because the membrane can be made much thinner than the detected wavelength, the antenna effectively radiates in free space, thus eliminating the substrate loss as well as the need for a dielectric lens. Measurements on log-periodic bismuth microbolometers deposited on a $1 \mu\text{m}$ silicon-oxynitride membrane show small sidelobes and a 3 dB beamwidth of 40° .¹² Because the thermometer is deposited on a thin membrane, the thermal conductance G is calculated in the two dimensional limit and, in general, will be lower than the three dimensional case, yielding a slower bolometer with a smaller NEP.

References

1. P. L. Richards, J. Clarke, R. Leoni, Ph. Lerch, S. Verghese, M. R. Beasley, T. H. Geballe, R. L. Hammond, P. Rosenthal, and S. R. Spielman, "Feasibility of the high T_c superconducting bolometer," *Appl. Phys. Lett.*, 54, 283-285, 1989.
2. Qing Hu and P. L. Richards, "Design analysis of a high T_c superconducting microbolometer," *Appl. Phys. Lett.*, 55, 2444-2446, 1989.
3. Tien-Lai Hwang, S. E. Swartz, and D. B. Rutledge,

"Microbolometers for infrared detection," *Appl. Phys. Lett.*, 34, 773-776, 1979.

4. D. B. Rutledge, D. P. Neikirk, and D. P. Kasilingam, "Integrated circuit antennas," *Infrared and Millimeter Waves*, edited by K. J. Button (Academic, New York), 1-90, 1983.

5. P. H. Siegel, "A planar log-periodic mixtenna for millimeter and submillimeter wavelengths," *IEEE Int. Microwave Symposium*, 649-652, 1986.

6. P. P. Tong, "Millimeter-wave integrated-circuit antenna arrays," Ph.D. thesis, California Institute of Technology, (Univ. Microfilms Intl., Ann Arbor, MI.) 1984.

7. *Thermophysical Properties of Matter*, edited by Y. S. Touloukian, 3rd ed. (Plenum, New York, 1977), Vol. 2.

8. *Thermophysical Properties of Matter*, edited by Y. S. Touloukian, 3rd ed. (Plenum, New York, 1980), Vol. 5.

9. *American Institute of Physics Handbook*, 3rd ed. (McGraw-Hill, New York, 1972), Chap. 9.

10. N. Newman, K. Char, S. M. Garrison, R. W. Barton, R. C. Taber, C. B. Eom, T. H. Geballe, and B. Wilkens, "YBCO superconducting films with low microwave surface resistance over large areas," *Appl. Phys. Lett.*, 57, 520-522, 1990.

11. It is assumed that G does not change significantly in the region of the resistive transition. This is verified by measuring the responsivity as a function of temperature and dividing by dR/dT .

12. G. M. Rebeiz, W. G. Regehr, D. B. Rutledge, R. L. Savage, C. W. Domier, and N. C. Luhmann Jr, "Submillimeter-wave antennas on thin membranes," *11th Intl. Conf. on Infrared and Millimeter Waves*, 1-3, 1986.

† Present address: Department of Electrical Engineering and Computer Science and Research Laboratory of Electronics, MIT.

* This work was supported by the Director, Office of Energy Research, Office of Basic Energy Sciences, Chemical Sciences Division, of the U. S. Department of Energy under Contract No. DE-AC03-76SF00098.

END

DATE FILMED

01 / 10 / 91

